UDC 621.3.013 https://doi.org/10.20998/2074-272X.2022.4.05

G. Merlin Suba, M. Kumaresan

Design of LLC resonant converter with silicon carbide MOSFET switches and nonlinear adaptive sliding controller for brushless DC motor system

Introduction. *The high voltage gain DC-DC converters are increasingly used in many power electronics application systems, due to their benefits of increased voltage output, reduced noise contents, uninterrupted power supply, and ensured system reliability. Most of the existing works are highly concentrated on developing the high voltage DC-DC converter and controller topologies for goal improving the steady state response of brushless DC motor driving system and also obtain the regulated voltage with increased power density and reduced harmonics, the LLC resonant DC-DC converter is implemented with the silicon carbide MOSFET switching devices* ***Problem****. Yet, it facing the major problems of increased switching loss, conduction loss, error outputs, time consumption, and reduced efficiency. Also the existing works are mainly concentrating on improving the voltage gain, regulation, and operating performance of the power system with reduced loss of factors by using the different types of converters and controlling techniques. The* ***goal*** *of this work is to obtain the improved voltage gain output with reduced loss factors and harmonic distortions.* ***Method****. Because, this type of converter has the ability to generate the high gain DC output voltage fed to the brushless DC motor with reduced harmonics and loss factors. Also, the nonlinear adaptive sliding controller is implemented to generate the controlling pulses for triggering the switching components properly. For this operation, the best gain parameters are selected based on the duty cycle, feedback DC voltage and current, and gain of silicon carbide MOSFET. By using this, the controlling signals are generated and given to the converter, which helps to control the brushless DC motor with steady state error.* ***Practical value****. The simulation results of the proposed LLC silicon carbide MOSFET incorporated with nonlinear adaptive sliding controller controlling scheme are validated and compared by using various evaluation indicators.* References 40, tables 3, figures 22.

Key words: **power conversion, brushless DC motor, silicon carbide MOSFET switches, LLC resonant converter, nonlinear adaptive sliding controller, voltage regulation harmonics suppression.**

Вступ*. Високовольтні перетворювачі постійного струму з високим коефіцієнтом посилення напруги все частіше використовуються в багатьох прикладних системах силової електроніки через їх переваги, пов'язані з підвищеною вихідною напругою, зниженим рівнем шуму, безперебійним живленням і гарантованою надійністю системи. Більшість існуючих робіт значною мірою зосереджені на розробці топологій високовольтного перетворювача постійного струму і контролера з метою поліпшення усталеного відгуку системи приводу безщіткового двигуна постійного струму, а також отримання регульованої напруги з підвищеною щільністю потужності і зменшеними гармоніками; резонансний LLC-перетворювач постійного струму, реалізований на перемикаючих пристроях на основі польових МОП-транзисторах з карбіду кремнію.* ***Проблема****. Тим не менш, це стикається з основними проблемами, пов'язаними зі збільшенням втрат при перемиканні, втратами провідності, помилками на виході, витратами часу та зниженням ефективності. Крім того, існуючі роботи в основному зосереджені на покращенні коефіцієнта посилення напруги, регулювання та робочих характеристик енергосистеми із зменшенням факторів втрат за рахунок використання різних типів перетворювачів та методів управління.* ***Метою*** *роботи є отримання покращеного коефіцієнта посилення напруги зі зниженими коефіцієнтами втрат і гармонійних спотворень.* ***Метод****. Таким чином, цей тип перетворювача здатний генерувати вихідну постійну напругу з високим коефіцієнтом посилення, що подається на безщітковий двигун постійного струму, зі зменшеними коефіцієнтами гармонік та втрат. Крім того, реалізований нелінійний адаптивний ковзний регулятор для генерування керуючих імпульсів для належного спрацьовування перемикаючих компонентів. Для цієї операції вибираються найкращі параметри посилення на основі робочого циклу, постійної напруги та струму зворотного зв'язку, а також коефіцієнта посилення польового МОП-транзистора з карбіду кремнію. При цьому керуючі сигнали генеруються і передаються на перетворювач, який допомагає керувати безщітковим двигуном постійного струму з помилкою, що встановилася.* ***Практична цінність****. Результати моделювання запропонованого LLC-перетворювача на основі польових МОП-транзисторів з карбіду кремнію зі схемою управління нелінійним адаптивним ковзним регулятором перевіряються та порівнюються з використанням різних показників оцінки.* Бібл. 40, табл. 3, рис. 22.

Ключові слова: **перетворення потужності, безщітковий двигун постійного струму, перемикачі на основі польових МОП-транзисторів, резонансний *LLC*-перетворювач, нелінійний адаптивний ковзний регулятор, придушення гармонік регулювання напруги.**

1. Introduction. In the recent days, the power electronics DC-DC converters [1-3] has gained a significant attention in many power application systems, due to their benefits of increased conversion efficiency, regulated voltage, reliability, uninterrupted power supply, and optimal cost consumption. When compared to the other DC-DC converters, the LLC resonant converter [4, 5] is more popular and increasingly used in the power electronics system like renewable energy sources, battery charging systems, plug-in electric vehicles and other low power applications. Because, the LLC converter [6, 7] could regulate the voltage gain based on the frequency of modulation. If the switching frequency of converter is matched with the resonance frequency [8, 9] it is determined as the circuit operations are efficient. Since, the LLC converter has the ability to efficiently reduce the switching as well as conduction losses. The modern power supply systems, DC micro-grids and high voltage DC power transmission systems [10, 11] widely utilized the LLC resonant converter due to its soft switching characteristics and increased density of power. Nevertheless, the conventional Si based converters [12, 13] facing difficulties related to the factors of high conduction loss, reduced switching frequency, and reduced voltage gain, which affects the efficiency and performance of entire power system.

Hence, the SiC-MOSFET [14-16] is one of the most suitable options for designing the LLC resonant converters, because it provides increased power outputs with reduced switching stress. Therefore, the proposed work intends to utilize the SiC-MOSFET [17] based inverter topology for efficiently controlling the brushless

DC (BLDC) motor system [18-20] with minimized harmonics distortions. Generally, the SiC-MOSFET circuitry has the major benefits of increased switching frequency, high speed in nature, ensured dynamic response, and minimized ripples. Hence, this work intends to utilize the SiC-MOSFET topology for controlling the BLDC motor [21, 22] system with the help of resonant DC-DC converter. For this purpose, a novel nonlinear adaptive sliding controller (NASC) mechanism is developed in this work, which is used to generate the controlling signals for actuating the SiC-MOSFET switching devices. This main objective of using this controlling mechanism is to control the speed and torque of BLDC motor based on the feedback signals. Also, the LLC resonant DC-DC converter is employed for regulating the random power obtained from the power source. The main intention of using this DC-DC converter is to efficiently boost the output power for charging batteries, and improving the performance of BLDC motor. The novel contributions of this works are two fold:

- to obtain the regulated voltage with increased power density and reduced harmonics, the LLC resonant DC-DC converter is implemented with the SiC-MOSFET switching devices;
- to improve the efficiency and controlling performance of BLDC motor, a novel NASC mechanism is developed;
- to attain the increased switching frequency, reduced error rate and optimal performance results, the mode of converter operations are properly performed according to the generated controlling signals;
- to assess the performance of proposed LLC-SiC MOSFET and NASC scheme, various evaluation indicators have been utilized.

2. Related works. This sector reviews some of the existing works related to the different types of converter and controller designs used in the power system applications based on its operating modes, key characteristics and functionalities. Also, it examines the benefits and limitations of the conventional converter and controlling techniques based on the factors of voltage gain, power conversion efficiency, controlling complexity, error rate, and harmonics.

In [23] was suggested a modulation based voltage control mechanism for controlling the speed of BLDC motor with the help of load resonant converter. Here, the main reason of using the LLC resonance converter circuit was to obtain the zero voltage switching with respect to varying switching conditions. It also objects to reduce the effect of electromagnetic interference noises with increased power density by using the LLC converter design. In [24] was designed a series resonant DC-DC converter topology for obtaining the improved voltage gain and power outputs based on the quality factor estimation. The key factor of this work was to reduce the switching losses by reduced loop inductance value. In [25] was suggested the LLC resonant converters with MOSFET switching devices for satisfying the requirements of high voltage applications. Here, the loss model of the converter design has been discussed, which includes both the conduction and switching loss factors. In addition to that, the key characteristics of Si-MOSFET and SiC-MOSFET switches were illustrated with its driving voltage speed. Based on this analysis, it was observed that the SiC-MOSFET switches provided the better performance outcomes in terms of increased voltage and speed, when compared to the Si-MOSFET switches. Also, the LLC converters could effectively reduce the loss factors by properly operating the mode of switching operations. In [26] was designed a power loss models with the LLC converter for optimally improving the level of system accuracy. Here, the time domain modelling could be adopted with this controlling strategy for obtaining increased power conversion efficiency. In [27] was provided the detailed overview about the design of LLC converters based on the synchronous rectification and power loss breakdown analysis. The key contribution of this work was to minimize the effect of duty loss by using the noise filtering circuit and the inclusion of phase compensation unit. In addition to that, the adaptive turnoff algorithm could be used to maximize the conduction time and to improve the performance of high speed digital controller. The different types of loss factors discussed in this work were copper loss, switching loss, core loss, diode and MOSFET conduction loss.

In [28] was developed a rotating coordinate system using the LLC resonant converter topology for obtaining the improved output dynamics. This paper discussed about the key benefits of using the LLC converter design, which includes high power density, better power conversion efficacy, minimal switching loss and increased switching frequency. Moreover, the state space analysis model was utilized for improving the design of LLC converter. In [29] was utilized the first harmonic approximation model with the H-bridge LLC converter for enhancing the stability and reliability of power conversion under varying load conditions. For this converter design, the MOSFET switching device was utilized to reduce both the voltage ripples and switching harmonics. The major benefit of this work was better system efficiency, stabilized output voltage, and minimal loss. In [30] was utilized a resonant LLC converter for obtaining an increased voltage gain. The main purpose of this work was to increase the gain of output voltage according to the quality factor, primary inductance, and secondary inductance value. Moreover, this circuit design was highly depends on the minimum and maximum voltage range. However, it limits with the major problems of increased error output, high harmonic contents, and complex design.

In [31] was developed a two stage LLC converter with SiC-MOSFET switching components for obtaining an increased voltage gain. Also, it objects to optimize the entire performance of converter with ensured peak efficiency and reduced harmonics. In [32] was implemented a voltage quadrupler rectifier incorporated with LLC converter for efficiently regulating the output voltage and improving the switching frequency. This work stated that the LLC converter could efficiently reduce the conduction and switching losses with normalized frequency outputs. In [33] was employed a power loss estimation model with LLC-MOSFET converter topology for efficiently minimizing the body diode, switching, and conduction losses. However, it limits with the issues of high controlling complexity, increased average error rate, and reduced power efficiency. In [34] was introduced a GaN based LCCL-LC controlling topology for improving the ability of fault ride through, improving the voltage regulation, and power density. Also, a multi-objective optimization methodology was utilized in this paper for designing the power transformer with reduced core and volume losses. In [35] was employed a multi-mode controlling strategy for enhancing the power conversion efficiency and density factors. The different types of factors mainly concentrated on this work were conduction loss, switching loss, driving loss, magnetic loss, and breakdown loss. It also intends to enhance the operating performance of controller under varying load conditions.

In [36] was introduced a medium voltage series resonant converter with SiC-MOSFET switching devices for solving the voltage imbalance issues. The key factor of this work was to design a new converter with reduced switching and conductance loss factors. In addition to that, it highly concentrated on protecting the circuit from over voltage, over current and over temperature issues. The main advantages of this work were regulated output voltage, reduced switching loss, and error output. Yet, it has the problems of high complexity in circuit design, inefficient output gain, and reduced power factor. In [37] was deployed a voltage sharing control scheme with the closed loop DC-DC converter for improving the voltage conversion efficiency of power systems. Here, the importance of using SiC-MOSFET switches have been discussed with respect to the parameters of voltage and current. Though, the major limitation of this work was reduced level of efficiency, which degrades the performance of entire system.

From this review, it is analyzed that the existing works are mainly concentrating on improving the voltage gain, regulation, and operating performance of the power system with reduced loss of factors by using the different types of converters and controlling techniques. But it facing the major problems of increased error outputs, high controlling complexity, harmonics distortions, and reduced switching frequencies. Hence, the proposed work intends to implement an LLC DC-DC converter with SiC-MOSFET switching devices and intelligent controlling technique for optimally improving the overall performance of system with reduced complexity.

3. Proposed methodology. This sector presents the clear description about the proposed converter and controlling scheme used for regulating the output voltage of the DC source with its equivalent circuit representations and algorithms.

The **goal** of this work is to obtain the improved voltage gain output with reduced loss factors and harmonic distortions. For this purpose, an advanced DC-DC converter and controlling techniques are developed, and the novel contribution of the proposed work is to design an intelligent NASC with the LLC resonant – SiC MOSFET DC-DC converter for controlling the speed of BLDC motor with improved voltage gain outputs.

The overall flow of the proposed model is depicted in Fig. 1, and its equivalent circuit representation is shown in Fig. 2.

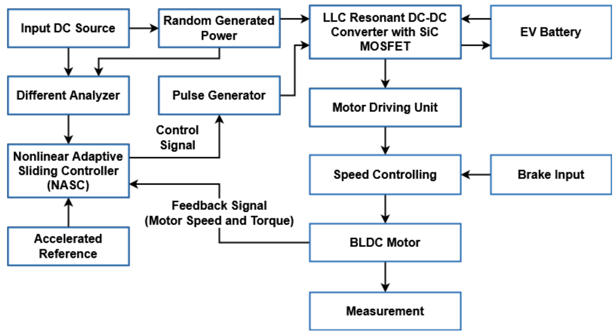

Fig. 1. Flow of the proposed LLC resonant with SiC-MOSFET and NASC controlling model

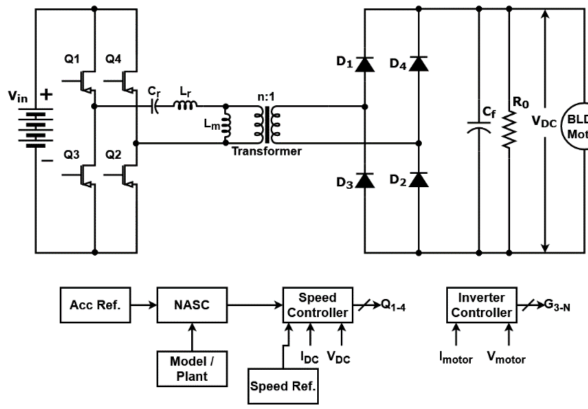

Fig. 2. Overall schematic representation

Typically, the power generated from the input DC source is an unregulated form, which must be regulated before giving it into the output load. Hence, the LLC resonant DC-DC converter incorporated with silicon carbide SiC-MOSFET switching devices are utilized in this model, which properly actuating the operating modes of switching components for boosting the voltage fed to the BLDC motor driving system. For efficiently generating the controlling signals to operate the switches of converter, the novel NASC controller scheme is developed in this work. It obtains the inputs of feedback signals from BLDC motor, accelerated reference, and output of different analyzer for generating the controlling signals with the help of pulse generator. Based on the generated controlling pulses, the LLC resonant converter can be operated for providing the maximum gain outputs to the motor driving system. The key benefits of this work are as follows: minimized controlling complexity, increased and regulated voltage gain output, minimal switching loss, conduction loss and harmonic contents.

A) LLC resonant – SiC MOSFET DC-DC converter. Conventionally, there are different types of resonant DC-DC converters are utilized for improving the voltage gain outputs, which includes the types of series resonant, parallel resonant and series-parallel resonant. In which, the LLC resonant DC-DC converter is widely used in different power application systems, due to its enormous benefits like simple designing, minimal losses, high operating efficiency, and increased voltage support. When compared to the Si-MOSFET switches, the SiC-MOSFET switches are the most option for designing the

LLC resonant converter, because it has the ability to operate under high switching frequencies with high efficiency. Also, the SiC-MOSFET switches are small in size, and it does not require any cooling necessities. Due to these facts, the proposed work intends to utilize the LLC resonant converter incorporated with the SiC-MOSFET switching devices for improving the efficiency and performance of BLDC motor system, and its equivalent circuit models are depicted in Fig 3,*a*,*b*.

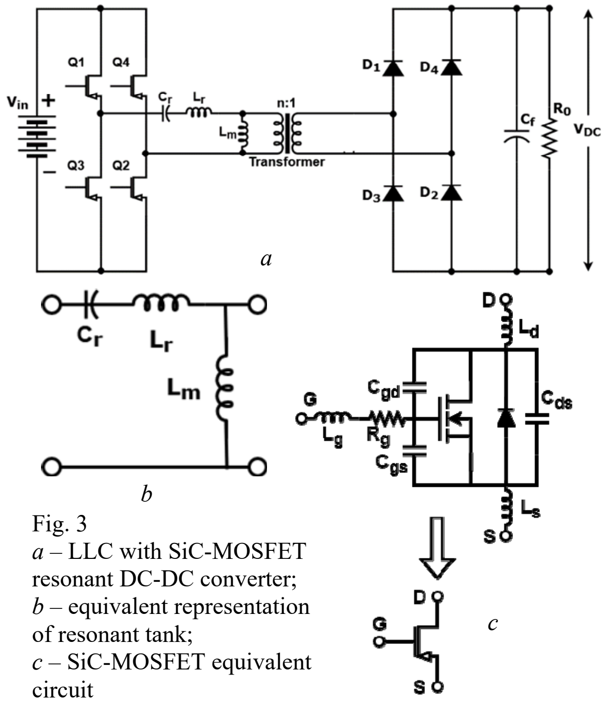

Fig. 3
a – LLC with SiC-MOSFET resonant DC-DC converter;
b – equivalent representation of resonant tank;
c – SiC-MOSFET equivalent circuit

As shown in Fig. 3,*c* the transfer function of SiC-MOSFET is determined as follows:

$$G(s)=\frac{\frac{1}{L_g\cdot C_{gg}}}{s^2+\frac{s\cdot R_g}{L_g}+\frac{1}{L_g\cdot C_{gg}}}\,, \qquad (1)$$

where s is the step signal; C_{gg} is the gate parallel capacitance; L_g is the line parasitic inductance; C_{gs} is the gate source capacitance; C_{gd} is the drain capacitance; R_g is the drive resistance.

The power for unit step $U_g(s)$ can be derived as:

$$U_g(s)=U_g/s\,. \qquad (2)$$

Consequently, the damping ratio is computed as follows:

$$\xi=\frac{R_g}{2}\cdot\sqrt{\frac{C_{gg}}{L_g}}\,. \qquad (3)$$

In this work the full-bridge LLC-SiC MOSFET DC-DC converter is mainly used to increase the voltage gain output with reduced harmonics fed to BLDC motor system. Typically, the LLC is a kind of the resonant converter that comprises the elements of inductors (L_r and L_m), capacitor (C_r), diodes (D_1 to D_4), and SiC-MOSFET switches (Q1 to Q4), and its equivalent circuit topology is shown in Fig. 3,*a*. In this model, there are 2 resonant frequencies have been gained with the combination of inductor L_r and capacitor C_r, and inductors (L_r, L_m) and capacitor (C_r), which are in the form of series arrangement. Then the frequencies of full bridge LLC resonant converter are estimated as follows:

$$f_{r1}=\frac{1}{2\pi\sqrt{L_r\cdot C_r}}\,; \qquad (4)$$

$$f_{r2}=\frac{1}{2\pi\sqrt{(L_r+L_m)\cdot C_r}}\,. \qquad (5)$$

The LLC resonant DC-DC converter's equivalent circuit mode of operations as 0 and 1 are illustrated in Fig. 4,*a*,*b*.

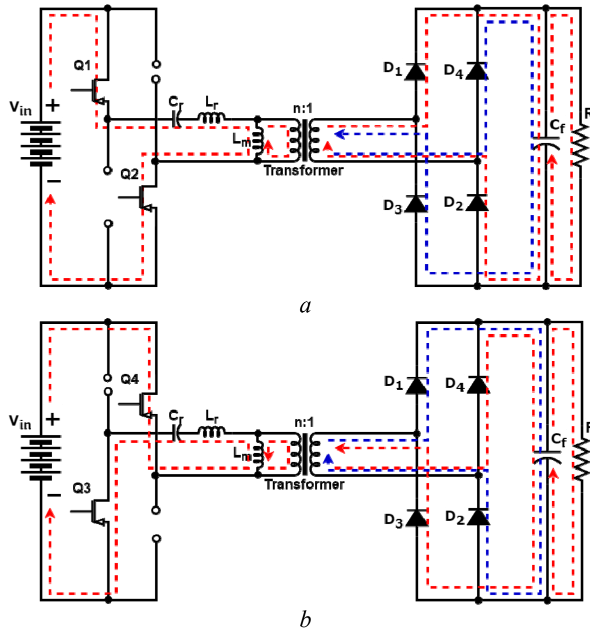

Fig. 4. *a* – operation mode 1 (Q1 & Q2 ON and Q3 & Q4 OFF);
b – operation mode 2 (Q1 & Q2 OFF and Q3 & Q4 ON)

Since, the LLC converter is working based on the functionality of inverter circuit at the input side of transformer. The switches Q1 and Q2 are turned ON and Q3 and A4 are turned off as shown in Fig. 4,*a*. This makes the capacitor C_r and the inductors L_r and L_m to charge up to the rated voltage, where the flow of current passes through the transformer. Then, the converter along with capacitor C_f to bypass the AC ripples, which provides the desired DC voltage at the load side.

In mode 2, the switches Q1 and Q2 are in OFF state and Q3 and Q4 are in ON state. At this time, the reverse current passes through the capacitor C_r and inductors L_r and L_m. This reverse flow of current also passes through the transformer and rectifier circuit. Since, this is a full bridge rectifier, hence it provides the constant DC voltage at the load side with C_f capacitor.

As shown in Fig. 5, the resonance induction ratio of RI_r and quality factor QF_L of the LLC resonant converter are calculated as follows:

$$RI_r=L_r/L_m\,; \qquad (6)$$

$$QF_L=R_i\cdot\sqrt{\frac{C_r}{L_r+L_m}}\,. \qquad (7)$$

According to the Kirchhoff's laws the output voltage and current are estimated as follows:

$$V_{ab}=i\cdot\left(A_{C_r}+A_{L_r}+A_{L_m}\right)-i_R\cdot X_{L_m}\,; \qquad (8)$$

$$i_R = \frac{i \cdot A_{L_m}}{\left(R_i + X_{L_m}\right)}; \quad (9)$$

$$i_R = \frac{n \cdot V_o}{R_i}, \quad (10)$$

where V_{ab} is the AC voltage generated from the inverter circuit of resonant converter; V_o is the output voltage; A is the temporary variable.

Based on (5), (6), the output value is obtained as follows:

$$i = \frac{n \cdot V_o \cdot \left(R_i + X_{L_m}\right)}{R_i \cdot X_{L_m}}. \quad (11)$$

Finally, the voltage gain of LLC resonant converter is expressed with respect to the ratio of output voltage and input voltage as illustrated in below:

$$\left|\frac{V_o}{V_i}\right| = \frac{1}{2n\sqrt{(1+RI_r)^2 \cdot \left(1-\left(\frac{\delta_L}{\delta}\right)^2\right)^2 + \left(\frac{1}{\delta_L}\right)^2 \cdot \left(\left(\frac{\delta}{\delta_L}\right) \cdot \left(\frac{RI_r}{1+RI_r}\right) - \left(\frac{\delta_L}{\delta}\right)\right)^2}}, \quad (12)$$

where V_i is the input voltage; RI_r is the resonance inductance ratio; δ, δ_L are the second resonant frequencies.

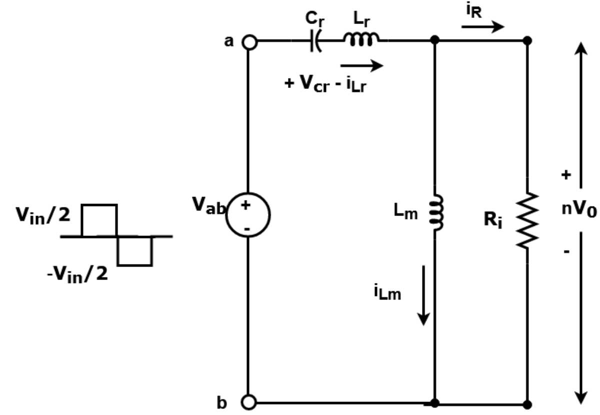

Fig. 5. Design properties of converter

B) Nonlinear adaptive sliding controller. The NASC algorithm is used to generate the controlling signals for operating the switching components of LLC resonant converter. This technique considers the inputs of converter parameters like duty cycle, feedback DC voltage, DC current, and gain parameters of SiC-MOSFET, and it produced output as the best selection of gain parameters. At first, the gain parameters are initialized with the maximum limits as indicated by K_p(max) and K_i(max), and the pitch ratio and harmonic limits are also initialized with the time instant. Then, the loop has been executed until reaching the maximum of iterations and number of decision parameter, where the random values are initialized as $r_1 = 1$ and $r_2 = 1$. If the harmonic rate (HR) is greater than the random value r_1, the gain parameters of K_p and K_i are updated as shown in below:

$$k_s = \left[k_p^{'}, k_i^{'}\right]. \quad (13)$$

Similar to that, of the pitch ratio (PR) is greater than the random value r_2, the new gain parameter is updated as represented below:

$$k_s^{'} = \left[\left(k_p^{'} + \text{rand}\right), \left(k_i^{'} + \text{rand}\right)\right]. \quad (14)$$

Otherwise, the new value is selected for updating the gain parameter, which is estimated as follows:

$$k_s^{'} = \text{rand} \times \left[\left(k_s(\text{upper}) - k_s(\text{lower})\right) + k_s(\text{lower})\right]. \quad (15)$$

Then, the convergence function is validated and the gain parameters are updated based on its maximum value, which is represented as follows:

$$k_s^{'} = k_s(i+1); \quad (16)$$

$$k_s^{'} = k_s(i). \quad (17)$$

Finally, the best selection of gain parameters are derived as indicated below:

$$K_p^{'} = k_s(t)[0]. \quad (18)$$

$$K_i^{'} = k_s(t)[1]. \quad (19)$$

Based on this value, the controlling pulses p' are generated and given to the converter for operating the switches to obtain the increased voltage output:

Algorithm: NASC controlling algorithm

Input: converter parameters (duty cycle, feedback DC voltage and current, gain parameter of SiC MOSFET)
Output: best selection of K_p, and K_i
Initialize gain parameters K and $K_{\max}$ and the maximum limit of K_p(max) and K_i(max) as $Z(k)$,
where $k_n \in K_n$, $\forall n = \{1, 2, ..., t\}$,
«t» – time instant / sample time.
initialize pitch ratio (PR), and harmonic rate (HR).
while ($i \le$ Max_iter), Do // Loop running for maximum number of iteration.
while ($j \le N$), Do // Loop running for number of decision parameter (N).
r_1 = rand(1); r_2 = rand(1) // Initialize random value for gain parameter.
If ($r_1 \le$ HR), then
Update the gain parameter of k_p and k_i by using (13);
If ($r_2 \le$ PR), then
Update the new gain parameter using (14);
End if
Else
Select new value of gain parameters by using (15);
End if
End «j» loop
Check for convergence function $F(t)^i$
If $F(t)^{i+1} < F(t)^i$, then
Compute k'_s by using (16);
Else
Compute k'_s by using (17);
End if
End «i» loop
Select K_p, and K_i as shown in (18) and (19) respectively;
Generate the pulse p' according to the gain parameters.

Finally, the generated high voltage DC output is fed to the BLDC motor driving system for improving its performance in terms of high torque and speed. The BLDC motor is a kind of synchronous motor system, which is widely used in many real time application systems like electric vehicles, automation industries, and medical sector. The major advantages of using the BLDC motor are fast dynamic response, increased speed and torque, improved operating efficiency, and minimal friction losses. Due to these facts, the proposed work intends to use the BLDC motor as the load unit for providing the increased voltage gain output.

Figure 6 shows the controlling structure of BLDC motor system used in the proposed model, where the magnetic field of both rotor and stator could be maintained at same frequency. For this motor, the DC output voltage is fed by the LLC resonant converter incorporated with SiC-MOSFET, where the DC output is transformed into three phase AC through the inverter circuit.

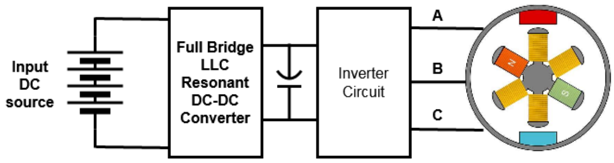

Fig. 6. BLDC driver

4. Results and discussion. This unit discusses about the performance analysis of the proposed controlling scheme by using various evaluation measures. Here, the simulation is performed with the help of MATLAB/Simulink tool, and scope results are illustrated according to the converter and controller circuits. Also, the obtained results are compared with some other recent state-of-the-art models for proving the efficiency and superiority of the proposed model.

A) Simulation analysis. Table 1 presents the performance analysis of the proposed LLC resonant DC-DC converter incorporated with SiC-MOSFET switches with respect to the measures of input voltage, output voltage, efficiency and gain. Based on this evaluation, it is assessed that the output voltage is efficiently increased with enhanced gain and efficiency measures. Because, the proposed NASC scheme could efficiently generating the controlling signals for properly actuating the switching modes of operations, which helps to increase the output voltage with high gain and efficiency values.

Table 1

Performance analysis of LLC resonant DC-DC converter

S. No	Input voltage, V	Output voltage, V	Gain	Efficiency, %
1	100	20.23	–11.68	50.2
2	200	38.66	–11.53	52.6
3	300	58.36	–11.25	53.5

Figure 7 shows the DC voltage obtained the DC input source with respect to varying time samples. This analysis shows that the minimum amount of voltage has been obtained from the DC source, which is in the form of unregulated voltage. So, it is efficiently regulated by using the LLC resonant converter in order to meet the requirements of BLDC motor. Consequently, the output DC voltage gain obtained from the converter is shown in Fig. 8 with respect to different time samples. This analysis proved that the obtained input voltage has been efficiently improved by using the DC-DC converter. Then, it can be fed to the BLDC motor driver system for controlling the speed with increased efficiency.

Figures 9, 10 show the output current of capacitor (C_f and C_r) with respect to corresponding varying time samples. Similarly, the current at inductor (I_r) is depicted under varying time sequences as depicted in Fig. 11, and final DC output current is shown in Fig. 12. The obtained results depict that the capacitor current could be effectively controlled by properly operating the switching components.

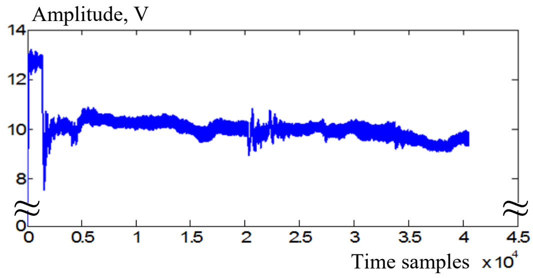

Fig. 7. DC voltage from input source

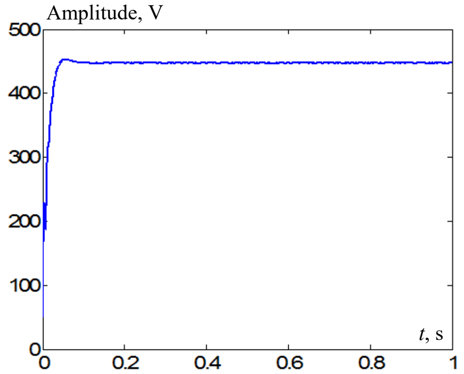

Fig. 8. Output DC voltage obtained from converter

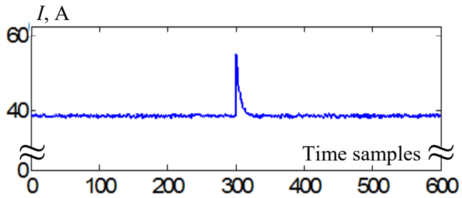

Fig. 9. Current at capacitor (C_f)

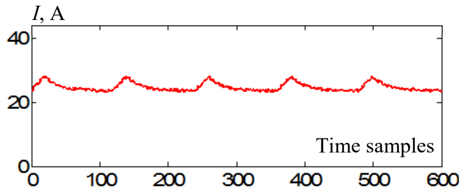

Fig. 10. Current at capacitor (C_r)

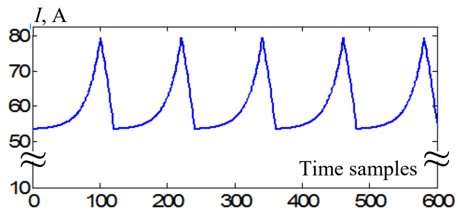

Fig. 11. Current at inductor (L_r)

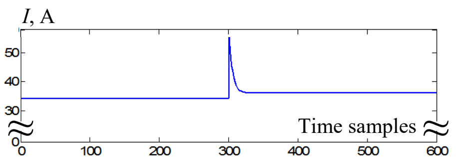

Fig. 12. DC current

Figure 13 illustrates the stator current of BLDC motor, and the results stated that the current is efficiently maintained under varying time instances. Also, the obtained results prove the improved performance and efficiency of the proposed converter and controlling scheme. Then, the generated gate pulses given to the converter by controlling unit is shown in Fig. 14, where the amplitude in volts is efficiently maintained according to the proper switching operations.

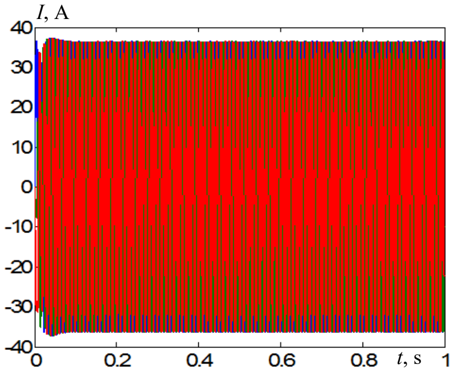

Fig. 13. Motor current

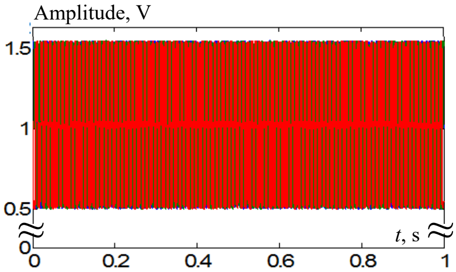

Fig. 14. Gate pulse

Figure 15 represents the step response of converter with respect to the amplitude (V) and time (s), and the generated waveform indicates that the time behavior characteristic of the proposed model is efficiently balanced with 0.5 V to 1 V.

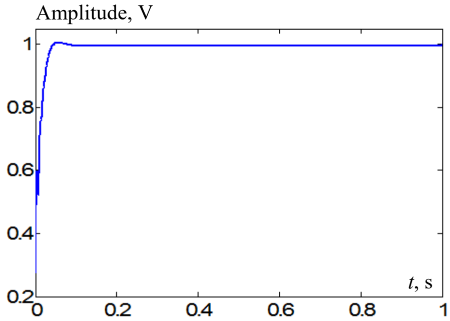

Fig. 15. Step response

Figure 16,*a*,*b* shows the motor speed and torque of the proposed LLC resonant integrated with NASC controlling mechanism with respect to varying time measures in terms of seconds correspondingly. Generally, the speed of motor drive system is highly depends on the generated switching pulses of controller. Also, controlling the speed of BLDC motor is more essential for driving the system at the required speed. The increased speed of motor is mainly correlated with the high gain voltage output generated by the converter. From this analysis, it is visibly perceived that the speed of BLDC motor is improved around 1500 rpm with increased voltage gain.

Figure 17 shows the overall efficiency analysis of the proposed LLC resonant with NASC scheme with respect to different time samples. Here, the efficiency of BLDC motor controlling is highly improved with the help of LLC resonant SiC MOSFET converter and NASC controlling technique. Since, it generates the regulated output voltage with high gain and reduced losses, which ensures the increased efficiency and optimal performance of the proposed system. Moreover, the THD analysis of the proposed scheme is validated according to the fundamental frequency. Due to the increased efficiency, high voltage gain output, and reduced losses, the THD level of the proposed converter and controlling scheme is competently reduced as shown in Fig. 18.

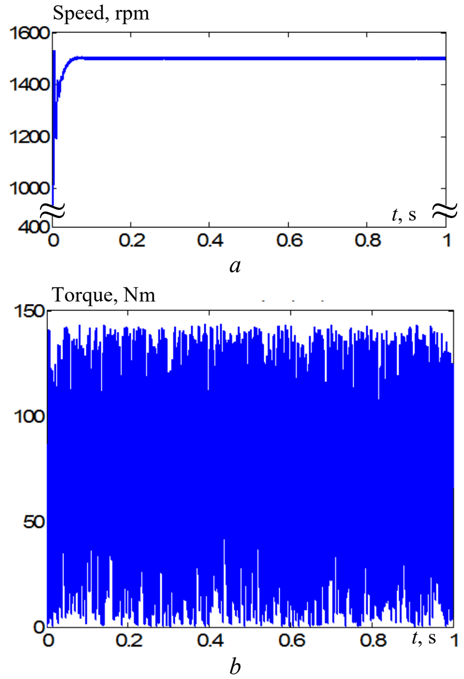

Fig. 16. *a* – motor speed; *b* – motor torque

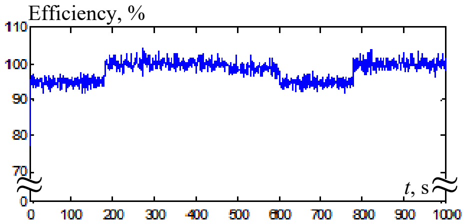

Fig. 17. Efficiency analysis

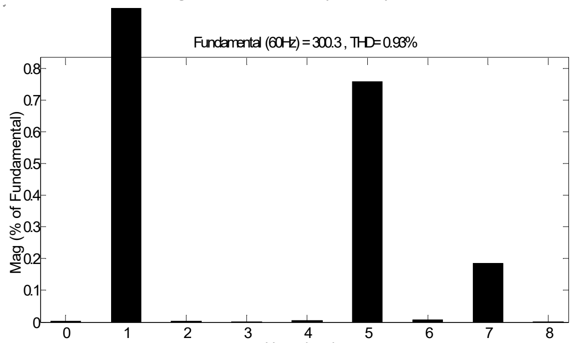

Fig. 18. THD analysis

C) Comparative analysis. Figure 19 compares the DC voltage gain of both conventional [38] and proposed converters under different duty cycles, which includes the topologies of step up DC-DC, multi-input DC-DC, boost DC-DC, and interleaved resonant PWM high step-up (IRPHS) DC-DC. In addition to that, the efficiency of converter is highly depends on the voltage gain output. Based on this evaluation, it is perceived that the voltage gain characteristics of the proposed LLC resonant – SiC MOSFET DC-DC converter is highly improved, when compared to the other converters. Moreover, the increased voltage gain of converter ensures the reduced conduction and switching losses of circuitry.

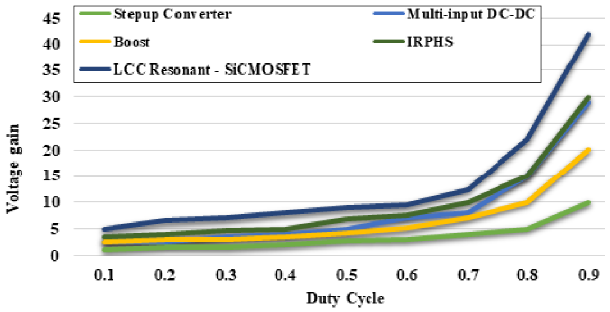

Fig. 19. Comparative analysis between various DC-DC converters based on the voltage gain

Consequently, the efficiency of existing IRPHS DC-DC and proposed LLC resonant – SiC MOSFET DC-DC converters are compared with respect to the output power as shown in Fig. 20. Due to the proper controlling of switching devices used in the converter, the efficiency of proposed converter has been highly improved under all output power values. The obtained results indicated that the proposed model achieved increased power conversion efficiency over the other technique.

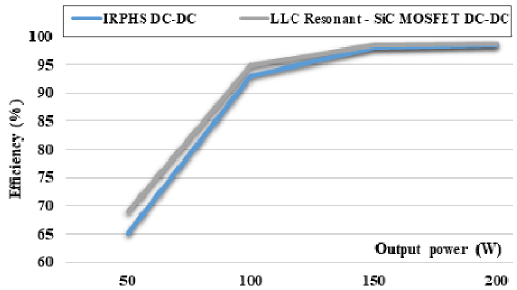

Fig. 20. Efficiency of existing and proposed converters

Figure 21 evaluates the voltage peak, settling time, and output voltage of the conventional [39] and proposed controlling techniques, in which the peak overshoot is estimated by analyzing that how much the level of peak value is increased compared to the steady state. Similarly, the settling time is defined as the amount of time of taken by the system for converging into the steady state. Based on this evaluation, it is analyzed that the voltage peak and settling time of the proposed model is efficiently reduced, and the output voltage is highly increased, when compared to the other controlling techniques. These results prove the improved performance and efficacy of the proposed technique over the other existing techniques.

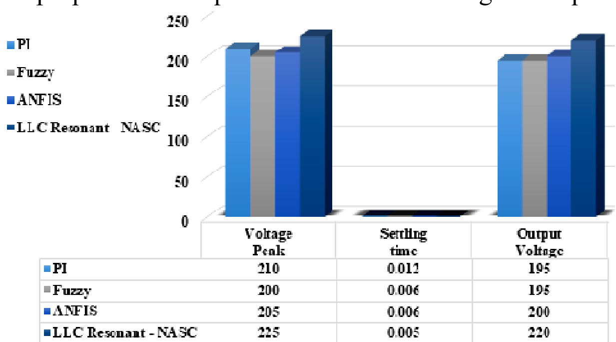

Fig. 21. Voltage peak, settling time and output voltage of existing and proposed controlling techniques

The rise time, peak time and peak value of the conventional controllers in [40] was proposed NASC controller are compared as shown in Table 2. When compared to these controlling mechanisms, the rise time, peak time and peak value of the proposed scheme is efficiently reduced based on the best selection of parameters for generating the controlling pulses. Moreover, the reduced time consumption ensures the improved performance of entire power conversion system.

Table 2

Comparative analysis based on time response

Controllers	Rise time, s	Peak time, s	Peak value, rpm
Anti-windup PID	0.4391	0.9987	1519.8
FLC	0.4024	0.9989	1517.1
Neuro-Fuzzy 1	0.4069	0.9981	1502.7
Neuro-Fuzzy 2	0.4121	1.0024	1500.6
BAT	0.4120	1.0009	1501
FPA	0.3785	1.0007	1500.7
Sugeno Fuzzy PID	0.3351	0.9971	1500
Proposed NASC	0.3245	0.9899	1500

Table 3 and Fig. 22 compare the time efficiency of conventional and proposed controlling techniques based on the parameters of peak overshoot, settling time, and steady state error. The obtained results proved that the proposed controlling technique provides the minimized peak overshoot, settling time, and steady state error, when compared to the other controlling schemes. Because, the power conversion efficiency of the proposed system is highly enhanced with reduced losses by selecting the optimal parameters for controlling the operating modes of switches. It helps to improve the system performance under varying load conditions with reduced error outputs.

Table 3

Comparative analysis of existing and proposed controlling schemes based on peak overshoot, settling time, and steady state error

Controllers	Peak overshoot, %	Settling time, s	Steady state error, %
Anti-windup PID	0.4963	0.6958	0.6391
FLC	0.1654	0.6549	0.6887
Neuro-Fuzzy 1	0.2334	0.6690	0.1749
Neuro-Fuzzy 2	0.2201	0.6664	0.3259
BAT	0.2200	0.6671	0.0647
FPA	0.0792	0.6243	0.0100
Sugeno Fuzzy PID	0.0216	0.5695	0.0061
Proposed NASC	0.0211	0.5280	0.0058

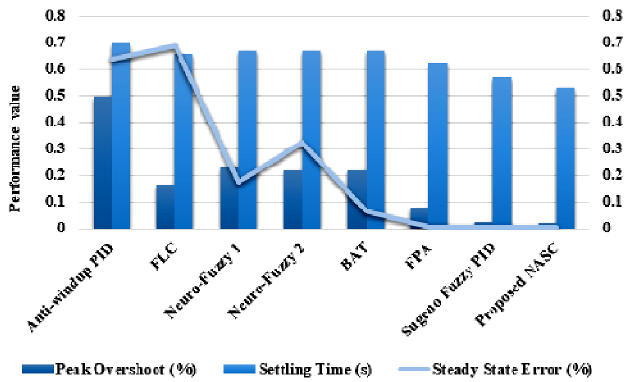

Fig. 22. Analysis of peak overshoot, settling time and steady state error

5. Future scope. As the future progresses, nonlinear adaptive sliding controllers will be replaced by genetic algorithms, neurofuzzy algorithms, or artificial intelligence systems. Additionally, SiC MOSFETs can be investigated in terms of their thermal resistance using the ON state voltage drop as a temperature-sensitive electrical parameter.

Conclusions. This paper developed an enhanced converter and controlling methodology for controlling the speed and improving the performance of brushless DC motor. For this purpose, the LLC resonant DC-DC converter incorporated with silicon carbide MOSFET switching device has been used for improving the voltage gain outputs with reduced harmonic distortions. Here, the main reason of using the silicon carbide MOSFET switching components are increased power outputs, reduced switching stress, fast dynamic response, and minimized ripples. Here, the novel nonlinear adaptive sliding controller mechanism is implemented to improve the efficiency and controlling performance of brushless DC motor with reduced conduction and switching losses. Also, it helps to obtain the increased switching frequency, reduced error rate and optimal performance results by properly generating the controlling signals in order to perform the mode of converter operations. For this operation, it acquires the input feedback signal, accelerated reference, and output of different analyzer for generating the controlling signals with the help of pulse generator. Then, it produced the best gain parameters as the output, which is used to generate the controlling signals. Finally, the obtained high gain voltage output is fed to the brushless DC motor system with reduced harmonics and losses. During simulation, the performance of conventional and proposed controlling topologies are validated and compared by using various evaluation measures. Based on the obtained results, it is evident that the proposed LLC resonant silicon carbide MOSFET incorporated with nonlinear adaptive sliding controller controlling scheme provided the better performance results over the other state-of-the-art models, which includes reduced error rate, peak overshoot, settling time, rise time and increased power conversion efficiency.

Conflict of interest. The authors of the paper state that there is no conflict of interest.

REFERENCES

1. Mukherjee S., Kumar A., Chakraborty S. Comparison of DAB and LLC DC–DC Converters in High-Step-Down Fixed-Conversion-Ratio (DCX) Applications. *IEEE Transactions on Power Electronics*, 2021, vol. 36, no. 4, pp. 4383-4398. doi: https://doi.org/10.1109/TPEL.2020.3019796.

2. Kumar G.K., Elangovan D. Review on fault-diagnosis and fault-tolerance for DC–DC converters. *IET Power Electronics*, 2020, vol. 13, no. 1, pp. 1-13. doi: https://doi.org/10.1049/iet-pel.2019.0672.

3. Jassim B.M., Jassim H. Modelling of a solar array simulator-based on multiple DC-DC converters. *International Journal of Renewable Energy Research*, 2018, vol. 8, no. 2, pp. 1038-1044. doi: https://doi.org/10.20508/ijrer.v8i2.6916.g7412.

4. Guan Y., Cecati C., Alonso J.M., Zhang Z. Review of High-Frequency High-Voltage-Conversion-Ratio DC–DC Converters. *IEEE Journal of Emerging and Selected Topics in Industrial Electronics*, 2021, vol. 2, no. 4, pp. 374-389. doi: https://doi.org/10.1109/JESTIE.2021.3051554.

5. Nie H., Bai Y., Cheng Q., Scott M.J. Evaluation of Conducted EMI in GaN and Si based Isolated DC/DC Converters. *2019 IEEE 7th Workshop on Wide Bandgap Power Devices and Applications (WiPDA)*, 2019, pp. 251-254. doi: https://doi.org/10.1109/WiPDA46397.2019.8998788.

6. Zhou X., Sheng B., Liu W., Chen Y., Wang L., Liu Y.-F., Sen P.C. A High-Efficiency High-Power-Density On-Board Low-Voltage DC–DC Converter for Electric Vehicles Application. *IEEE Transactions on Power Electronics*, 2021, vol. 36, no. 11, pp. 12781–12794. doi: https://doi.org/10.1109/TPEL.2021.3076773.

7. Salem M., Ramachandaramurthy V.K., Jusoh A., Padmanaban S., Kamarol M., Teh J., Ishak D. Three-Phase Series Resonant DC-DC Boost Converter With Double LLC Resonant Tanks and Variable Frequency Control. *IEEE Access*, 2020, vol. 8, pp. 22386-22399. doi: https://doi.org/10.1109/ACCESS.2020.2969546.

8. Rouzbehi K., Miranian A., Escaño J.M., Rakhshani E., Shariati N., Pouresmaeil E. A Data-Driven Based Voltage Control Strategy for DC-DC Converters: Application to DC Microgrid. *Electronics*, 2019, vol. 8, no. 5, p. 493. doi: https://doi.org/10.3390/electronics8050493.

9. Dhanalakshmi R., Usha Rani P. A Review on Two-Stage Back End DC-DC Converters in On-Board Battery Charger for Electric Vehicle. *International Journal of Renewable Energy Research*, 2020, vol. 10, no. 4. pp. 1685-1695. doi: https://doi.org/10.20508/ijrer.v10i4.11181.g8054.

10. Yang X., Cheng Zhang Y., Wen P., Liu Y., Zheng T.Q., Takaku T., Igarashi S. Improved Phase Shift Control for SiC-MOSFET Based Resonant Switched-Capacitor Converter With Parasitics Consideration. *IEEE Transactions on Industry Applications*, 2020, vol. 56, no. 4, pp. 3995-4006. doi: https://doi.org/10.1109/TIA.2020.2989389.

11. Manikandan R., Raja Singh R., Edison G., Gnanaraj S.D. Hardware-in-Loop-Based Reliability Improvement of Power Converter for Critical Electrical Drive Applications. In: Priyadarshi N., Bhoi A.K., Bansal R.C., Kalam A. (eds) *DC-DC Converters for Future Renewable Energy Systems. Energy Systems in Electrical Engineering*, 2022, Springer, Singapore. doi: https://doi.org/10.1007/978-981-16-4388-0_14.

12. Kawa A., Stala R. SiC-Based Bidirectional Multilevel High-Voltage Gain Switched-Capacitor Resonant Converter with Improved Efficiency. *Energies*, 2020, vol. 13, no. 10, p. 2445. doi: https://doi.org/10.3390/en13102445.

13. Monopoli V.G., Sidella P., Cupertino F. A Si-IGBT-Based Solution to Drive High-Speed Electrical Machines. *IEEE Transactions on Industry Applications*, 2019, vol. 55, no. 5, pp. 4900-4909. doi: https://doi.org/10.1109/TIA.2019.2919821.

14. Nakahara M., Kawaguchi Y., Furukawa K., Kadota M., Mabuchi Y., Kanoda A. Development of a Control Method for LLC Converter Utilized for Input-Parallel-Output-Series Inverter System with Solid-State Transformers. *IEEJ Journal of Industry Applications*, 2019, vol. 8, no. 4, pp. 652-659. doi: https://doi.org/10.1541/ieejjia.8.652.

15. Frivaldský I.M., Drgoňa P., Špánik P. Experimental analysis and optimization of key parameters of ZVS mode and its application in the proposed LLC converter designed for distributed power system application. *International Journal of Electrical Power & Energy Systems*, 2013, vol. 47, pp. 448-456. doi: https://doi.org/10.1016/j.ijepes.2012.11.016.

16. Chakraborty S., Vu H.-N., Hasan M.M., Tran D.-D., Baghdadi M.El, Hegazy O. DC-DC Converter Topologies for Electric Vehicles, Plug-in Hybrid Electric Vehicles and Fast Charging Stations: State of the Art and Future Trends. *Energies*, 2019, vol. 12, no. 8, p. 1569. doi: https://doi.org/10.3390/en12081569.

17. Li Y., Liang M., Chen J., Zheng T.Q., Guo H. A Low Gate Turn-OFF Impedance Driver for Suppressing Crosstalk of SiC MOSFET Based on Different Discrete Packages. *IEEE Journal of Emerging and Selected Topics in Power Electronics*, 2019, vol. 7, no. 1, pp. 353-365. doi: https://doi.org/10.1109/JESTPE.2018.2877968.

18. Rahul Charles C.M., Savier J.S. Bidirectional DC-DC Converter Fed BLDC Motor in Electric Vehicle. *2021 International Conference on Advances in Electrical, Computing, Communication and Sustainable Technologies (ICAECT)*, 2021, pp. 1-6. doi: https://doi.org/10.1109/ICAECT49130.2021.9392394.

19. Darcy Gnana Jegha A., Subathra M.S.P., Manoj Kumar N., Subramaniam U., Padmanaban S. A High Gain DC-DC Converter with Grey Wolf Optimizer Based MPPT Algorithm

for PV Fed BLDC Motor Drive. *Applied Sciences*, 2020, vol. 10, no. 8, p. 2797. doi: https://doi.org/10.3390/app10082797.
20. Nikhila M., Saritha E. Solar PV fed Common Grounded Z-Source DC-DC Converter based BLDC Motor Drive. *In proceedings of the International Conference on Systems, Energy & Environment (ICSEE) 2019*, GCE Kannur, Kerala, July 2019, doi: https://doi.org/10.2139/ssrn.3447745.
21. Dineshkumar S., Sachinamreiss G. Control and optimal design of DC – DC converter of electric vehicle fed by BLDC motor drive. *International Journal of Recent Technology and Engineering*, 2019, vol. 8, no. 1, pp. 1557-1560. Available at: https://www.ijrte.org/wp-content/uploads/papers/v8i1/A1115058119.pdf (accessed 11 May 2021).
22. Karthikeyan B., Kalyanasundaram V., Vidyasagar S., Sundararaju K., Palanisamy R. FFNN based MPPT controller for PEMFC powered non-isolated high gain DC-DC converter with SPWM inverter fed BLDC motor. *IOP Conference Series: Materials Science and Engineering*, 2021, vol. 1055, no. 1, p. 012147. doi: https://doi.org/10.1088/1757-899X/1055/1/012147.
23. Riczeena Jose, Santhi B. Simulation of Pulse Amplitude Modulation based Voltage Control Technique for the Speed Control of BLDC Motor using Class-E Load Resonant Converter. *International Journal of Engineering Research & Technology*, 2015, vol. 4, no. 9, pp. 516-518. doi: https://doi.org/10.17577/IJERTV4IS090593.
24. Shen Y., Wang H., Al-Durra A., Qin Z., Blaabjerg F. A Structure-Reconfigurable Series Resonant DC–DC Converter With Wide-Input and Configurable-Output Voltages. *IEEE Transactions on Industry Applications*, 2019, vol. 55, no. 2, pp. 1752-1764. doi: https://doi.org/10.1109/TIA.2018.2883263.
25. Chen G., Li H., Sun X., Zhou J., Bai L. Analysis and design of LLC converter based on SiC MOSFET. *2018 13th IEEE Conference on Industrial Electronics and Applications (ICIEA)*, 2018, pp. 1443-1448. doi: https://doi.org/10.1109/ICIEA.2018.8397936.
26. Wei Y., Mantooth A. Experimental Validations of the SiC MOSFET based LLC Converter Circuit and Power Loss Models. *2021 IEEE 8th Workshop on Wide Bandgap Power Devices and Applications (WiPDA)*, 2021, pp. 322-327. doi: https://doi.org/10.1109/WiPDA49284.2021.9645112.
27. Wei Y., Luo Q., Mantooth H.A. Synchronous Rectification for LLC Resonant Converter: An Overview. *IEEE Transactions on Power Electronics*, 2021, vol. 36, no. 6, pp. 7264-7280. doi: https://doi.org/10.1109/TPEL.2020.3040603.
28. Cao S., Zhang Y., Zheng C. High Efficiency LLC Converter Design Using a novel Modelling Method based on SiC MOSFET. *2019 22nd International Conference on Electrical Machines and Systems (ICEMS)*, 2019, pp. 1-5. doi: https://doi.org/10.1109/ICEMS.2019.8921615.
29. Han P., He X., Ren H., Zhao Z., Peng X. Research on High Efficiency LLC DC-DC Converter Based on SiC MosFet. *2018 International Power Electronics Conference (IPEC-Niigata 2018 - ECCE Asia)*, 2018, pp. 2714-2717. doi: https://doi.org/10.23919/IPEC.2018.8507508.
30. Dimitrov B., Sharkh S., Cruden A., Balabozov I. Implementation of a DC current sensing transformer with H-bridge MOSFET rectifier in a resonant LLC converter. *2018 20th International Symposium on Electrical Apparatus and Technologies (SIELA)*, 2018, pp. 1-4. doi: https://doi.org/10.1109/SIELA.2018.8447120.
31. Wang F., Wang X., Ruan X. An Optimal Design Scheme of Intermediate Bus Voltage for two-stage LLC Resonant Converter Based on SiC MOSFET. *2021 IEEE Workshop on Wide Bandgap Power Devices and Applications in Asia (WiPDA Asia)*, 2021, pp. 488-492. doi: https://doi.org/10.1109/WiPDAAsia51810.2021.9655998.
32. Shang M., Wang H. A Voltage Quadrupler Rectifier Based Pulsewidth Modulated LLC Converter With Wide Output Range. *IEEE Transactions on Industry Applications*, 2018, vol. 54, no. 6, pp. 6159-6168. doi: https://doi.org/10.1109/TIA.2018.2850033.
33. Glitz E.S., Ordonez M. MOSFET Power Loss Estimation in LLC Resonant Converters: Time Interval Analysis. *IEEE Transactions on Power Electronics*, 2019, vol. 34, no. 12, pp. 11964-11980. doi: https://doi.org/10.1109/TPEL.2019.2909903.
34. Hu J., Wang J., Burgos R., Wen B., Boroyevich D. High-Density Current-Transformer-Based Gate-Drive Power Supply With Reinforced Isolation for 10-kV SiC MOSFET Modules. *IEEE Journal of Emerging and Selected Topics in Power Electronics*, 2020, vol. 8, no. 3, pp. 2217-2226. doi: https://doi.org/10.1109/JESTPE.2019.2943742.
35. Sha D., Zhang J., Sun T. Multimode Control Strategy for SiC mosfets Based Semi-Dual Active Bridge DC–DC Converter. *IEEE Transactions on Power Electronics*, 2019, vol. 34, no. 6, pp. 5476-5486. doi: https://doi.org/10.1109/TPEL.2018.2866700.
36. Lu Z., Li C., Zhu A., Luo H., Li C., Li W., He X. Medium Voltage Soft-Switching DC/DC Converter With Series-Connected SiC MOSFETs. *IEEE Transactions on Power Electronics*, 2021, vol. 36, no. 2, pp. 1451-1462. doi: https://doi.org/10.1109/TPEL.2020.3007225.
37. Qu L., Zhang D. Input voltage sharing control scheme for input series and output series DC/DC converters using paralleled MOSFETs. *IET Power Electronics*, 2018, vol. 11, no. 2, pp. 382-390. doi: https://doi.org/10.1049/iet-pel.2017.0519.
38. Karthikeyan B., Sundararaju K., Palanisamy R. ANN-Based MPPT Controller for PEM Fuel Cell Energized Interleaved Resonant PWM High Step Up DC-DC Converter with SVPWM Inverter Fed Induction Motor Drive. *Iranian Journal of Science and Technology, Transactions of Electrical Engineering*, 2021, vol. 45, no. 3, pp. 861-877. doi: https://doi.org/10.1007/s40998-021-00413-0.
39. Rajani B., Bapayya Naidu K. Renewable Source DCMicrogrid Connected BLDC Water Pumping System with Adaptive Control Techniques. *2020 4th International Conference on Electronics, Communication and Aerospace Technology (ICECA)*, 2020, pp. 216-222. doi: https://doi.org/10.1109/ICECA49313.2020.9297486.
40. Karuppannan A., Muthusamy M. Wavelet neural learning-based type-2 fuzzy PID controller for speed regulation in BLDC motor. *Neural Computing and Applications*, 2021, vol. 33, no. 20, pp. 13481-13503. doi: https://doi.org/10.1007/s00521-021-05971-2.

Received 06.03.2022
Accepted 26.05.2022
Published 20.07.2022

G. Merlin Suba[1], *Research Scholar,*
M. Kumaresan[1], *Professor,*
[1] Department of Electrical and Electronics Engineering,
Dr. M.G.R Educational and Research Institute,
Maduravoyal, Chennai 600095, Tamil Nadu, India,
e-mail: merlinsubagphd@gmail.com (Corresponding author);
dr.kumaresn09@gmail.com

How to cite this article:
Merlin Suba G., Kumaresan M. Design of LLC resonant converter with silicon carbide MOSFET switches and nonlinear adaptive sliding controller for brushless DC motor system. *Electrical Engineering & Electromechanics*, 2022, no. 4, pp. 34-43. doi: https://doi.org/10.20998/2074-272X.2022.4.05